

Exploiting Semantic Localization in Highly Dynamic Wireless Networks using Deep Homoscedastic Domain Adaptation

Lei Chu, *Senior Member, IEEE*, Abdullah Alghafis, and Andreas F. Molisch, *Fellow, IEEE*

Abstract—Localization in GPS-denied outdoor locations, such as street canyons in an urban or metropolitan environment, has many applications. Machine Learning (ML) is widely used to tackle this critical problem. One challenge lies in the mixture of line-of-sight (LOS), obstructed LOS (OLOS), and non-LOS (NLOS) conditions. In this paper, we consider a semantic localization that treats these three propagation conditions as the "semantic objects", and aims to determine them together with the actual localization, and show that this increases accuracy and robustness. Furthermore, the propagation conditions are highly dynamic, since obstruction by cars or trucks can change the channel state information (CSI) at a fixed location over time. We therefore consider the blockage by such dynamic objects as another semantic state. Based on these considerations, we formulate the semantic localization with a joint task (coordinates regression and semantics classification) learning problem. Another problem created by the dynamics is the fact that each location may be characterized by a number of different CSIs. To avoid the need for excessive amount of labeled training data, we propose a multi-task deep domain adaptation (DA) based localization technique, training neural networks with a limited number of labeled samples and numerous unlabeled ones. Besides, we introduce novel scenario adaptive learning strategies to ensure efficient representation learning and successful knowledge transfer. Finally, we use Bayesian theory for uncertainty modeling of the importance weights in each task, reducing the need for time-consuming parameter finetuning; furthermore, with some mild assumptions, we derive the related log-likelihood for the joint task and present the deep homoscedastic DA based localization method. Extensive simulations with a 3D ray tracing dataset demonstrate that identifying environmental semantics and the proposed DA localization schemes significantly improve the accuracy of localization methods in many challenging scenarios.

Index Terms—Semantic Localization, Time-varying Environmental Semantics, Channel State Information, Multi-task Bayesian Learning, Homoscedastic Domain Adaptation.

I. INTRODUCTION

LOCALIZATION is becoming an increasingly important part of cellular systems, both because it forms the basis for improved cellular operation (e.g., for planning of handovers), and as a service underlying applications such as intelligent transportation systems. While 5G foresees various ways for "classical" (e.g., time-of-arrival based) localization, and Beyond 5G (B5G) offers even further expanding opportunities for localization

methods [1]–[5], much of the current interest in this field has turned to machine-learning (ML) based localization.

In this paper, we investigate the demanding localization of users in street canyons in urban areas, which are crucial in intelligent transportation systems, but pose a number of special challenges: (i) they are GPS-denied, thus necessitating a purely cellular solution for localization, (ii) they show high dynamics of the channel state information (CSI) even at fixed locations, due to the movement of vehicles and other objects that can act as scatterers or blockage [6], [7]. Consequently, classical localization methods, such as fingerprinting, or trilateration (based on the existence of a line-of-sight LOS), might fail. As a result, this paper considers ML-based localization algorithms that are model-free and can learn novel representations for the data in those scenarios.

II. RELATED WORKS

A. Deep Learning based Localization

Localization based on deep learning has been shown to improve accuracy and reliability. Consequently, there is a large number of papers on this topic, see, e.g., the surveys [8]–[10] and references therein. While many investigations are based on received power only, there have also been investigations into the use of the full channel state information (CSI), i.e., the transfer function or impulse response, possibly observed at multiple antenna elements (or corresponding information in the angular domain). Compared to power-only based localization methods, the fine-grained CSI is more robust for the multi-path fading and temporal dynamics [11]. Besides, the CSI [12] and its variants [13], [14] contain detailed information for multi-path characteristics and are thus compatible with a deep structure in the neural network (NN) [8]. In deep learning, many types of neural networks [10], [13] have been employed to represent the fingerprints and offer an end-to-end relationship between the fingerprints and the coordinate(s) of the user(s). For example, [12] utilized a multiple-layer NN to represent CSI fingerprints, yielding profitable results in two representative indoor environments. Besides, [14] considered the convolutional neural network and took input as the angular delay profiles (ADP), whose sparsity nature boosts feature extraction. In summary, deep

learning technologies pave a new way for localization by providing novel representation for the sampled RF data, building an end-to-end nonlinear relationship between the CSI data and coordinates, and realizing the goal of single-site localization.

B. Deep Domain Adaptation based Transfer Learning for the Enhanced Localization in the Dynamic Environment

A special challenge of wireless localization based on supervised ML or fingerprinting is that the environment may change between the measurement of the training data and the desired localization. Thus, accommodating time-varying environments is an important goal in algorithm design [10], [15]. To deal with this challenging issue, earlier works [16], [17] proposed to utilize transfer learning (TL). The related TL-based localization algorithms successfully apply to received signal strength (RSS) data collected over space, devices, and time. Later works [18], [19] employed the CSI data and offered advanced TL methods to improve the robustness of localization against environmental dynamics and other practical constraints. However, those novel methods were conducted in an inductive way, in which the network models were trained offline with existing data and retrained with fresh ones. The inductive TL requires online labeled data collection, hindering its practical applications.

On the other hand, collecting unlabeled data offers more flexibility. DA based TL techniques [20] enable localizing user(s) accurately and adaptively by utilizing unlabeled RF data, which can be collected easily and cheaply. In the literature, DA methods [21]–[27] were used to improve the scalability and robustness of localization algorithms in a transductive way. For example, [21] formulated the DA framework based on variational auto-encoders (VAE). The VAE-based DA localization method integrates data argumentation and adaptive knowledge transfer, realizing sub-meter level indoor localization with WIFI CSI data. Moreover, our conference paper [25] proposed a new adversarial regressive domain adaptation (RDA) method to localize user(s) in a GPS-denied outdoor environment with high dynamics. It adopted an adversarial learning scheme and advanced a nonlinear location regressor to improve the robustness against the environmental changes and the scalability of location space, respectively. Although those methods provide promising localization results, they do not fully take advantage of B5G wireless networks. It is appealing to renovate the localization method with deep learning and B5G wireless networks.

C. Semantic Localization

The classical model-based localization methods are susceptible to the existence of the LOS path and the number of multi-path components (MPCs). For the dynamic scenario, the moving vehicles would temporarily/spatially block the LOS and add/block some non-line of sight (NLOS) path(s). As a result, it is demanding

yet essential to reconsider the model-based method and exploit a new way, i.e., semantic localization, in this work. Compared to the classical localization setting, semantic localization [28]–[31] adds the new dimension of location information – semantics in the context [29]. For example, [28] boosts localization performance by incorporating visual semantics, which helps to discard ambiguous features. [30] employs the semantic sub-region (e.g., a conference room in the indoor environment) to perform location disambiguation. We note that most semantic localization works have been done for indoor environments, where the semantic context usually refers to the location in a specific room.

However, localization with the above *static* semantics is still insufficient in many practical situations, such as GPS-denied and dynamic outdoor environments. The receiver(s) will experience time-varying propagation conditions in a realistic environment caused by moving object(s) between the transmitter and receiver, leading to a dynamic number and amplitude of MPCs. In this work, we take advantage of the CSI and exploit semantic localization for these challenging areas, in which the semantics refers to the main propagation conditions, namely the amount of blockage of the LOS component. What's more, the rapid development of wireless networks, such as the B5G cellular network, allows us to understand and analyze the environmental dynamics [32] and the ML methods lead to deeper insights [33].

D. Contribution

This paper considers both the static and dynamic environmental semantics and aims to make the neural network aware of these semantics, striving to realize robust and accurate localization in such a tricky wireless environment. The key contributions are as follows:

- We introduce the propagation condition as a novel indicator for the time-varying environmental semantics and formulate semantic localization as a multi-task learning problem. We note that while for propagation researchers, it might seem obvious that the LOS condition impacts the CSI, to our knowledge, this condition has not yet been directly included in any deep learning-based end-to-end localization algorithms.
- We propose a multi-task domain adaptation (MDA) based localization scheme, including scenario-adaptive supervised loss functions and novel knowledge alignment designs, which enable the neural network to learn good representations for the CSI with both labeled and unlabeled data. The scenario-adaptive knowledge alignment design offers efficient and effective knowledge transfer from labeled data to unlabeled one, improving the robustness of the localization algorithm against environmental changes. Furthermore, to reduce the time-consuming parameter finetuning in the MDA method, we employ the homoscedastic uncertainty

measure in the Bayesian theory to represent the importance weights of each task. Moreover, with some mild assumptions, we attain the log-likelihood of the joint task and solve the problem with the maximum likelihood inference criterion.

- We conduct comprehensive case studies¹ based on a 3D ray tracing dataset, and the experimental results show that semantic localization provides significant improvements compared to the classical one in highly dynamic scenarios. Besides, the proposed localization methods outperform the robustness and accuracy of competing ones in all investigated system configurations.

E. Paper organization and Notations

The remainder of this paper is organized as follows. Section III introduces the semantic localization in wireless networks, including the system model and the problem formulation. Then, in Section IV, we first elaborate on the proposed MDA localization method and designs of the loss function. Besides, we introduce the improved version to improve the overall robustness. Next, Section V extensively compares the proposed localization algorithms with existing ones in different system configurations. Lastly, conclusions are presented in Section VI.

We use bold lower-/upper- case to denote vectors/matrices. The hatted vectors and matrices ($\hat{\mathbf{x}}, \hat{\mathbf{X}}$) refer to their estimates; the notation $\|\cdot\|$ over a vector/matrix means the related L_2 /spectral norm. We use \mathbb{E} to denote the expectation function. The symbols Ω and $|\Omega|$ represent the data ensemble and its length. The notations Ω^S/\mathcal{W}^S and Ω^T/\mathcal{W}^T mean the dataset/parameters in source-domain and target-domain, respectively. Let \mathbf{x} and \mathcal{W} be the input and neural network parameters (weights and bias), respectively. Then the neural network function will be denoted by $f_{\mathcal{W}}(\mathbf{x})$. The notation $a \propto b$ means a is linearly proportional to b . We use \otimes and \odot to denote the Kronecker and Hadamard products.

III. SEMANTIC LOCALIZATION IN WIRELESS NETWORKS: PROBLEM FORMULATION AND THEORETICAL INSIGHT

A. Channel Model and Localization Problem

This work focuses on object positioning, such as pedestrian and self-driving vehicles, in a street canyon, a typical outdoor GPS-denied area of the intelligent transportation system. We consider a MISO (multiple-input single-output) downlink, such that a user equipment (UE) with a single, possibly omnidirectional, antenna receives transmissions from a base station (BS) using OFDM modulation. The BS antenna is a uniform planar array with M_y and M_z elements and half-wavelength spacing in horizontal and vertical directions, with $M = M_y M_z$. We assume that the UE can receive the transmit

signal from the BS via P paths (MPCs), and each MPC is characterized by complex gain α_p , the direction of departure (elevation angle θ_p , and azimuth angle ϕ_p), and delay τ_p . Then the channel frequency response (CFR) [11] \mathbf{h}_k on the k -th subcarrier can be denoted by

$$\mathbf{h}[f_k] = \sum_{p=1}^P \alpha_p \mathbf{a}(\phi_p, \theta_p, f_k) e^{-j2\pi f_k \tau_p} \quad (1)$$

where $\mathbf{a}(\phi_p, \theta_p, f_k)$ is the array steering vector of dimension $M \times 1$, evaluated at the frequency f_k and along the direction (ϕ_p, θ_p) . Given K available subcarriers and assuming no beam squinting exists (so that \mathbf{a} becomes independent of f), the complete channel state information (CSI) combines all K sub-carriers CFR: $\mathbf{H} = [\mathbf{h}[f_1], \dots, \mathbf{h}[f_K]] \in \mathbb{C}^{M \times N}$. For the localization problem based on the channel model (1), model-based algorithms can use the related CSI measurements to infer the distances or the angles between the BS and UE(s) and then apply a simple geometric calculation to get the estimates of coordinates of the UE(s) [34]. In our case studies, the moving vehicles will bring in two significant impacts: 1) They may temporally block the Line-of-sight (LOS) path; 2) They may temporally and spatially create/block some new non-LOS path(s). For the channel model in Eq. (1), those impacts are related to the case that the first path may not exist, or we can have a variable number of MPCs (P in Eq. (1)). With the model and through its combined modeling, simulation, and post-processing capabilities, Wireless Insite software provides efficient and accurate predictions of EM propagation and communication channel characteristics in complex urban, indoor, rural, and mixed-path environments.

B. Semantic Localization

Localization algorithms are sensitive to environmental dynamics. For example, a slight movement of the UE(s) and/or movement of environmental scatterers will make the phases of the complex amplitudes $\arg(\alpha_p)$ vary over space; the $|\alpha_p|$, (ϕ_p, θ_p) , and τ_p , also change (though more slowly) with the movement of the UE(s). Besides, moving environmental objects, e.g., vehicles, can block MPCs and thus cause significant variations of the absolute amplitudes and may also result in a varying number of MPCs. As a result, it is indispensable to exploit new avenues to robust localization in wireless networks with high dynamics.

Following the concepts of the modeling theory [31], one can use a structure $\langle \mathbf{P}, \mathbf{d} \rangle$ to represent the model of the space of semantic localization. The elements of \mathbf{P} refer to the location-related information while the ones of \mathbf{d} provide the spatially meaningful interpretations, i.e., visual semantics [28] and subregion index [30].

In this work, based on experimental studies [25], [35], we use the real-time propagation conditions indicators to denote the time-varying geometrical semantics. For example, in real scenarios, the related propagation conditions [35] include 1) LOS case, in which the LOS path

¹To enable reproducibility, the related codes will be released on the project website: <https://github.com/Leo-Chu/SemanticLoc>

exists; 2) obstructed line-of-sight (OLOS), where some geometrically sparse objects, i.e., trees, block the LOS path; 3) NLOS, in which the buildings surrounding the UE(s) block the LOS path. For the employed ray tracing scenarios in the deepMIMO dataset [6], the propagation conditions include: 1)LOS; 2)NLOS; 3) Full blockage, which includes no path between the BS and the UE(s). Note that the LOS and NLOS distinction depends on the location of the UE and is (for a given location) time-invariant, while the classification of blockage and no-blockage is time-variant.

C. Model-based Semantic Localization: Joint Propagation Condition Prediction and Location Estimation

We start this section by introducing the semantic localization problem with an exact statistical CSI model, with which we can define the location estimation and related propagation conditions prediction straightforwardly. Many statistics exist to determine the propagation conditions [33]. We employ the delay information in this work to indicate the propagation conditions. Given Γ CSI measurements $\{\tilde{\mathbf{H}}_t\}_{1, \dots, \Gamma}$, we are interested in solving a joint estimation problem:

$$(\hat{\phi}_p, \hat{\theta}_p, \hat{\tau}_p) = \arg \min \sum_{t=1}^{\Gamma} \|\mathbf{H}_t(\phi_p, \theta_p, \tau_p) - \tilde{\mathbf{H}}_t\|_F^2. \quad (2)$$

A popular solution to the problem is the space-alternating generalized expectation maximization (SAGE) algorithm [36]. With SAGE, one can estimate the related MPCs, i.e., $\hat{\phi}_p, \hat{\theta}_p, \hat{\tau}_p$ in (2). Then one can easily apply a simple geometric calculation to get estimates of UE(s)'s coordinates and predefined thresholds (based on the estimated delays) to infer the accompanying propagation conditions [34].

With the exact statistical channel model, the advantage of joint (delay and angle information) estimation over solo estimation has been broadly verified in the literature [37]–[40]. For indoor localization, the static semantics can be directly used to enhance the K-nearest neighbor (KNN) algorithm [41], which is widely adopted for the final step of location estimation. Furthermore, one can easily verify the related advantage in a practical double-direction channel, with which the transmitter(s) send the signals to the receiver(s) [42]. When the transmitter(s) and receiver(s) come from the same direction, the angles are insufficient to separate MPCs, thus providing accurate location estimation. On the other hand, the delay(s) helps to distinguish the MPCs from the same angles. However, no off-the-shelf semantics exist in dynamic outdoor scenarios, which motivates us to exploit a new way to figure out the appropriate semantics in such an environment.

IV. JOINT BLOCKAGE PREDICTION AND LOCALIZATION: PROPOSED METHODS

The joint estimation problem (2) is based on a precise mathematical relationship between the CSI measure-

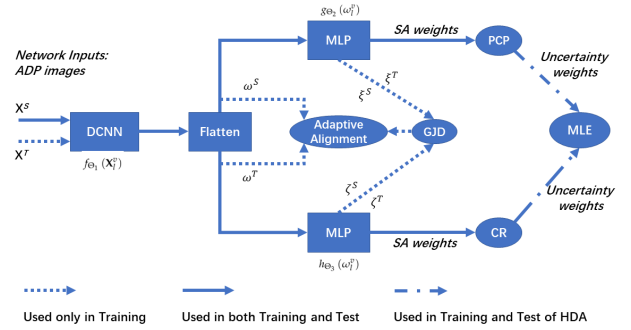


Fig. 1: The overall architecture of the proposed method.

ments and MPCs. However, due to the high environmental dynamics, it is appealing to solve the problem by alternative methods that require no precise signal model and antenna calibration and high computational burdens of the expectation maximization algorithms. Primarily, we treat the semantic localization problem in a collaborative task form:

- 1)Coordinates Regression (CR) Task:

$$\{x, y, z\} \xleftrightarrow{\text{NN}} \text{CSI} \quad (3)$$

- 2) Propagation Condition Prediction (PCP) Task. In Eq. (4), based on the real-scene experiments [35] or ray-tracing dataset [6], we only consider three propagation conditions as the time-varying geometrical semantics. It is noted that the proposed localization method has no constriction for the types/numbers of propagation conditions.:

$$I(\mathbf{H}) = \begin{cases} 0 & \text{LOS path exists} \\ 1 & \text{OLOS path exists} \\ 2 & \text{All NLOS paths} \end{cases} \quad (4)$$

We use a neural network (NN) to learn the relationship between the CSI and UE's coordinates by tackling a nonlinear regression problem. At the same time, with the indicator functional $I(\mathbf{H})$, the NN can also identify the propagation condition by solving a classification problem. We employ the propagation condition as the environmental semantics and solve the related localization problem with a novel multi-task deep learning framework, which will be introduced in the following.

A. On the Multi-task Deep Unsupervised Domain Adaptation based Solution

In this paper, we provide novel localization methods based on the unsupervised DA framework [43], in which the related deep learning algorithms can learn a unified representation for both labeled and unlabeled data, strengthening the robustness against the effect of high environmental dynamics. Our following designs are motivated by joint estimation [37], [38], [40], and multi-task DA theory [44]. In detail, for the joint tasks in (3) and (4), we first provide a multi-task deep unsupervised domain adaptation (MDA)-based solution.

1) *Method Overview*: As shown in Fig. 1, we consider the task of unsupervised DA for semantic localization. In this setting, we assume that we have data pairs in the source domain, $\Omega^S = \{\mathbf{X}_l^S, \mathbf{z}_l^S\}_{l=1, \dots, |\Omega^S|}$, and the target domain, $\Omega^T = \{\mathbf{X}_l^T\}_{l=1, \dots, |\Omega^T|}$, where $|\Omega^S|$ and $|\Omega^T|$ are the number of available data samples in each domain. In this paper, \mathbf{z} is a vector of dimension 4×1 , where the first three elements of \mathbf{z} are the coordinates of the UE's location (denoted by \mathbf{y}) and the last the environmental semantics (the indicator of the propagation condition, denoted by d). The network input \mathbf{X} denotes the angle-delay domain channel power matrix [14], which can be denoted by

$$\mathbf{X} \triangleq \mathbf{G} \odot \mathbf{G}^* \in \mathbb{R}^{M \times N}, \quad (5)$$

where

$$\mathbf{G} \triangleq \frac{1}{\sqrt{MN}} \left(\mathbf{V}_{M_y}^H \otimes \mathbf{V}_{M_z}^H \right) \mathbf{H} \mathbf{F}^* \in \mathbb{C}^{M \times N}, \quad (6)$$

$[\mathbf{F}_N]_{i,k} = \frac{1}{\sqrt{N}} e^{-j2\pi \frac{ik}{N}}$ is the (i, k) -th element of the *unitary* discrete Fourier transform (DFT) matrix $\mathbf{F}_N \in \mathbb{C}^{N \times N}$, and $\mathbf{V}_M \in \mathbb{C}^{M \times M}$ denotes a phase-shifted DFT matrix with the (i, k) -th element being $[\mathbf{V}_M]_{i,k} = \frac{1}{\sqrt{M}} e^{-j2\pi \frac{i(k-M/2)}{M}}$. The ADP matrices sparsely represent critical features of CSI, making them excellent input candidates that are well suited for the learning process [13], [14]. Please see Sec. V-D for more types of CSI measurements.

Our goal is to design a hybrid task neural networks that can reliably and accurately estimate the coordinates of UE(s) and indicate the propagation condition for each CSI measurement (or its variants) in the target domain. To achieve this goal, we present an end-to-end trainable neural network, which contains three main network modules: 1) Feature extraction network f , parameterized by Θ_1 ; 2) Nonlinear location regression network g , parameterized by Θ_2 ; 3) Propagation condition classification network h , parameterized by Θ_3 . The objective function \mathcal{L} for training the proposed network includes four loss terms and is defined as

$$\mathcal{L}_{MDA} = \lambda_1 \mathcal{L}_{CR} + \lambda_2 \mathcal{L}_{PCP} + \lambda_3 \mathcal{L}_{KT} + \lambda_4 \mathcal{L}_{WR}, \quad (7)$$

where $\{\lambda_k\}_{k=1,2,3,4}$ are the hyperparameters used to control the importance of each loss term. \mathcal{L}_{CR} is used to estimate the coordinates of UE(s) while \mathcal{L}_{PCP} to identify the corresponding environmental semantics. These two tasks share the feature extraction module. The scenario-adaptive knowledge alignment loss \mathcal{L}_{KT} is designed to adaptively optimize the neural network with the help of unlabeled data and semantic identification. \mathcal{L}_{WR} is an auxiliary task to enhance the stability of neural network training. We will elaborate on each loss function in the following.

2) *Scenario-Adaptive Supervised Loss Function for the Joint Task*: To solve the problem shown in Eq. (3) and Eq. (4), a natural choice is to use the multiple task learning method, in which we first employ a neural network f_{Θ_1} to perform the feature extraction for the inputs \mathbf{X}_l^v , $v \in \{S, T\}$, yielding an output as $\{\omega_v\}_{v \in \{S, T\}} = f_{\Theta_1}(\mathbf{X}_l^v)$. After that, for the CR task, we use the least square error (L2) loss

function to minimize the squared differences between the true coordinates and predicted ones:

$$\begin{aligned} \mathcal{L}_{CR} &= \min_{\Theta_1, \Theta_2} \mathbb{E}_{\{\mathbf{X}^S, \mathbf{y}^S\} \in \Omega^S} L_2(\Theta_1, \Theta_2) \\ &= \min_{\Theta_1, \Theta_2} \frac{1}{|\Omega^S|} \sum_l \|\zeta_l^v - \mathbf{y}_l^S\|_2^2. \end{aligned} \quad (8)$$

Furthermore, we calculate the modulated cross-entropy (CE) loss (also known as the focal loss) [45] between the PCP task predictions and corresponding ground truth labels d_l as

$$\begin{aligned} \mathcal{L}_{PCP} &= \min_{\Theta_1, \Theta_3} \mathbb{E}_{\{\mathbf{X}^S, d^S\} \in \Omega^S} L_{CE}(\Theta_1, \Theta_3) \\ &= \min_{\Theta_1, \Theta_3} \frac{1}{|\Omega^S|} \sum_l CE\left(- (1 - \xi_l^v)^\gamma \log \xi_l^v, d_l^S\right). \end{aligned} \quad (9)$$

The loss functions in (8) and (9) are used for training f_{Θ_1} and the two specific networks g_{Θ_2} and h_{Θ_3} with labeled data. For brevity of notation, in (8) and (9), we have $\zeta_l^v = g_{\Theta_2}(\omega_l^v)$, $\xi_l^v = h_{\Theta_3}(\omega_l^v)$, $v \in \{S\}$. $(1 - \xi^v)^\gamma$ is the modulating factor [45] with the non-negative number γ being its *temperature*, which is also known as the focusing parameter. The loss \mathcal{L}_{PCP} is equivalent to the vanilla CE when $\gamma = 0$. The loss function shown in (9) is meaningful in practice. Consider a case with semantic label 1 (NLOS CSI samples), and ξ_l^v small, then the modulating factor is near 1, which means the loss \mathcal{L}_{PCP} is unaffected. On the other hand, when we have a case with the semantic label being 0, during the training process, the modulating factor goes to zero ($\xi_l^v \rightarrow 1$), and the loss for LOS CSI samples is down-weighted. As a result, with the modulated CE loss (9), the network optimization will be conducted in an adaptive way, granting more weights for NLOS (hard to learn) samples. Assigning different importance weights for examples with different semantic labels is one of the key designs for semantic localization.

3) *Scenario-Adaptive Knowledge Alignment Loss Function*: Based on the framework of deep unsupervised DA, our goal is to align the knowledge learned from labeled data to unlabeled ones. The popular implementations minimize the distance between learning representations from the source and target domains. For example, the distance measure [43] can be Maximum Mean Discrepancy, Kullback–Leibler (KL) divergence, and their variants. In our case, for data in the source and target domains, we have one local representation $\{\omega^v\}_{v \in \{S, T\}}$ and two global representations: $g_{\Theta_2}(\omega^v)$ and $h_{\Theta_3}(\omega^v)$.

However, for semantic localization, fully matching the whole distributions of source and target CSI measurements to each other at the global level may not be effective, as domains could have scene layouts, i.e., different moving vehicle positions. On the other hand, adaptive alignment yields superior performance based on recent advances in DA theory and related applications [46], [47]. For example, the strong-weak distribution alignment [47], and adversarial matching strategies [46] significantly improve the DA algorithms' performance in objection detection and image recognition tasks. This motivates us to propose a scenario adaptive knowledge

alignment for semantic localization. We first employ the symmetrical Kullback–Leibler (SKL) divergence to align the local features, which can be denoted by

$$L_{loc} = \arg \min_{\Theta_1} \mathbb{E}_{\mathbf{X} \in \{\Omega^S \cup \Omega^T\}} SKL(\omega^S, \omega^T), \quad (10)$$

where

$$SKL(\omega^S, \omega^T) = D_{KL}(\omega^S || \omega^T) + D_{KL}(\omega^T || \omega^S),$$

$$\omega^v = \frac{P'_v}{\sum P'_v}, P'_v = \frac{1}{|\Omega^v|} \sum_l \omega_l^v, v \in \{S, T\},$$

and $D_{KL}(P||Q) = \sum_i P(i) \ln \frac{P(i)}{Q(i)}$.

For the global feature alignment, we have

$$L_{global} = \arg \min_{\{\Theta_1, \Theta_2, \Theta_3\}} \mathbb{E}_{\mathbf{X} \in \{\Omega^S \cup \Omega^T\}} SKL(\Phi_{\otimes}(\xi^S, \zeta^S), \Phi_{\otimes}(\xi^T, \zeta^T)), \quad (11)$$

where \otimes denotes the Kronecker product, and we use the modulated multilinear condition map [48] to get the joint distribution of global representations in the CR and PCP task:

$$\Phi_{\otimes}(\xi^v, \zeta^v) = -(1 - \xi^v)^\gamma \log(\xi^v) \otimes \zeta^v, v \in \{S, T\}. \quad (12)$$

The multilinear condition map (12) captures the global multi-modal conformation behind complex data distributions [46]. Besides, it is designed to put more weight on the NLOS samples than the LOS ones during the training and to dominate the distribution of global representation in the PCP task with LOS samples, making this novel map scenario adaptive. Since the SKL is a convex function in the domain of probability distributions, the alignment based on the SKL is also scenario adaptive.

Putting everything together, we get the scenario adaptive knowledge alignment loss function as

$$\mathcal{L}_{KT} = L_{global} + L_{loc}. \quad (13)$$

Lastly, we use auxiliary weights regularization (WR),

$$L_{WR} = \arg \min_{\Theta = \{\Theta_1, \Theta_2, \Theta_3\}} \mathbb{E}_{\mathbf{X} \in \{\Omega^S \cup \Omega^T\}} \frac{1}{2} \|\Theta\|_2^2$$

to avoid over-fitting and enhance the robustness of deep neural network models [49].

B. Semantic Localization With Homoscedastic Domain Adaptation

1) *Motivations*: As shown in Fig. 2, we empirically found that the performance of the localization algorithm is highly dependent on the relative weights between each dominant (supervised) task loss (\mathcal{L}_{CR} , \mathcal{L}_{PCP}). One should manually fine-tune these weights to get the best performance with different communication system configurations, increasing the computational burden. Therefore, we will focus on the method that can simultaneously learn to balance the regression and classification tasks with various conditions.

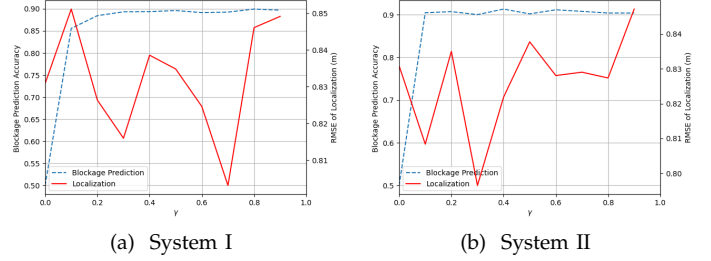


Fig. 2: The performance variation of the proposed semantic localization algorithm (MDA) over different values of λ . Here, we assume $\lambda_1 + \lambda_2 = 1$ and leave out the subscript for simplicity. Case I and Case II denote a communication system with the related bandwidth being 100M and 500M, respectively.

2) *Maximum Likelihood Estimation in the Joint Task*: To solve this challenging issue, we employ the related Bayesian learning theory [50] to model the weights (also known as the relative confidence) in the CR and PCP tasks with some uncertainty measures, which will be elaborated in the following. Since these weights are task-independent, the corresponding uncertainty measures and the knowledge transfer technology will be referred to as Homoscedastic uncertainty [50] and Homoscedastic domain adaptation (HDA). Our goal is to obtain the likelihood function of the joint task, as shown in Section IV-A2. We make some mild assumptions about the network outputs to tackle this tricky issue.

Assumption 1: Let \mathbf{x} and \mathbf{y} be the input data and corresponding labels of a neural network g , parameterized by \mathcal{W}_1 . Denoting the random output of the network model as $g_{\mathcal{W}_1}(\mathbf{x})$, then the model likelihood is given by $p(\mathbf{y}|g_{\mathcal{W}_1}(\mathbf{x}))$. For regression tasks, one can define the likelihood as a Gaussian with the mean given by the model output [50]

$$p(\mathbf{y}|g_{\mathcal{W}_1}(\mathbf{x})) = \mathcal{N}(g_{\mathcal{W}_1}(\mathbf{x}), \sigma_1^2), \quad (14)$$

with σ_1^2 being an observation noise scalar.

Assumption 2: Let \mathbf{x} be the input of a multiple-task neural network with K outputs, denoted by $\{\mathbf{y}_k\}_{k=1, \dots, K}$. These outputs are independent events.

Following the analysis in Section IV-A, the learnable network parameter ensembles in the PCP and CR tasks are denoted by $\mathcal{W}_1 = \{\Theta_1, \Theta_2\}$, $\mathcal{W}_2 = \{\Theta_1, \Theta_3\}$, respectively. The unknown variable σ_1^2 will be learned during the optimization. With these mild assumptions, we can obtain the following result.

Theorem 1: Let Θ be the learnable parameters ensemble in the investigated neural network. The network model's outputs constitute a continuous output \mathbf{y}_1 (CR task) and a discrete one \mathbf{y}_2 (PCP task with standard CE loss). The related log-likelihood of the joint task can be given by:

$$\log p(\mathbf{y}_1, \mathbf{y}_2 | f_{\Theta}(\mathbf{x})) \propto -\frac{1}{2\sigma_1^2} \mathcal{L}_1 - \frac{1}{\sigma_2^2} \mathcal{L}_2 - \log \sigma_1 - \log \sigma_2^2, \quad (15)$$

where $L_1 = \|\mathbf{y}_1 - g_{w_1}(\mathbf{x})\|^2$, and $L_2 = -\log \text{softmax}(h_{w_2}(\mathbf{x}))$, $\{\sigma_k\}_{k=1,2}$ are some learnable probability rescaling factors.

Corollary 1: Let $\mathbf{u} = h_{w_2}(\mathbf{x})$, for a joint task neural network with \mathbf{y}_1 and \mathbf{y}_2 being its outputs, applying modulated CE loss in the PCP task yields a log-likelihood as:

$$\begin{aligned} & \log p(\mathbf{y}_1, \mathbf{y}_2 = c | f_{\Theta}(\mathbf{x})) \\ & \propto -\frac{1}{2\sigma_1^2} \|\mathbf{y}_1 - f_{w_1}(\mathbf{x})\|^2 - \log \sigma_1 - \log \sigma_2^2 \\ & + \left(1 - \frac{1}{\sigma_2} \text{softmax}(\mathbf{u})^{\frac{1}{\sigma_2}}\right)^{\gamma} \log(\text{softmax}(\mathbf{u})), \end{aligned} \quad (16)$$

The proof is given in the Appendices. We have two remarks based on Theorem 1 and Corollary 1.

Remark 1: The log-likelihood of the joint task ((15) or (16)) is a linear combination of the loss functions \mathcal{L}_{PCP} and \mathcal{L}_{CR} .

Remark 2: With the mean squared error (MSE) criterion, the optimization is implemented by minimizing the MSE of the targets and related estimates. Similarly, in the maximum likelihood inference, one can maximize the log-likelihood of the model. In the literature, these two optimization schemes are effective for a similar optimization target with different principles [51].

In this work, we employ the maximum likelihood principle to perform optimization for a joint task neural network while measuring the uncertainty of each task with two learnable probability rescaling factors. The factor σ_1 in the CR task captures how much noise we have in the outputs, while σ_2 in the PCP task describes the confidence of the predictions [52]. Minimization of σ_1 and σ_2 are related to surpassing the noise and alleviating the negative effect of overconfident predictions.

3) *Overall Loss:* With Theorem 1, we will cooperatively optimize the neural network by minimizing the negative log-likelihood of the joint task (Eq. (16)). Besides, the relative confidence for the CR and PCP tasks are determined by two learnable parameters σ_1 and σ_2 and will be optimized during the whole algorithm optimization. We use the same knowledge alignment loss function and weight regularization shown in Section. IV-A. Based on the above analysis, we finally get the overall loss for the proposed HDA localization method, denoted by

$$\mathcal{L}_{HDA} = \min_{\{\Theta, \sigma_1, \sigma_2\}} -\log p(\mathbf{y}_1, \mathbf{y}_2 = c | f_{\Theta}(\mathbf{x})) + \lambda_3 \mathcal{L}_{KT} + \lambda_4 \mathcal{L}_{WR}. \quad (17)$$

The MDA method is designed for the novel idea of semantic localization, which adds wireless semantics analysis to assist the localization in a challenging environment (with high dynamics and weak GPS signals). We first solve related semantic localization with the MDA method, which integrates two independent tasks with the unsupervised DA framework. Furthermore, to avoid using a naive weighted sum of supervised (dominant) losses or manually tuning the related weights, we propose the HDA method, which combines multiple loss functions with homoscedastic task uncertainty. Comparing the design shown in (7), (17) only adds two more learnable parameters. However, it significantly reduces

the computational complexity of the MDA method in wireless networks with several changeable system parameters, such as time-varying MPCs, bandwidths, and carrying frequencies.

V. CASE STUDIES

This section elaborates on case studies in which the implementation of neural networks and related datasets is foremost introduced. After this, we evaluate the performance of all deep learning models with different communication systems and the various conditions that affect the dataset. Lastly, we assess the efficiency of deep learning methods by showing the convergence and complexity analysis.

A. The Neural Network Implementation, Dataset, and Evaluation Protocols

1) *Implementation Details:* We implement our network model using Pytorch and train the network using Google Colab with up to 52GB GPU memory. To enable fair comparison, we use a similar network structure as in [13] to perform feature extraction (Θ_1) for all compared methods. The structure of Θ_1 consists of four convolutional layers, each followed by a 2D batch normalization functional, max pooling, and a ReLU activation. For the non-linear location regression network Θ_2 and the propagation condition classification Θ_3 , we use the Multilayer perceptron (MLP) structure. We employ three MLP layers, in which the first two MLPs include one linear mapping layer, 1D batch normalization functional, and a ReLU activation. The last layer in Θ_2 has no nonlinear activation function, while the one in Θ_3 has a Sigmoid activation function. All neural networks are initialized with the Xavier initialization scheme [49]. For the input CSI data, we perform antennas-wise normalization, with which the maximum of the CSI vector at each antenna element is set to unity. The following section will discuss more types of normalization. During the training process, we have a batch size of 256, a learning rate of 10^{-3} with the momentum being 0.99, and set the weight decay as 10^{-4} .

The determination of the hyperparameters in the proposed MDA method is based on the manual optimization scheme, in which we manually optimize λ_1 and λ_2 from 0.0 to 1.0 with a step size being 0.1; we obtain an approximately optimal weight (denoted by Approx. opt.) as $\lambda_1 = 0.3, \lambda_2 = 0.7$. For the proposed HDA method, the related weights can be automatically optimized thanks to the theoretical analysis. For the weights of the task L_{KT} , following the work of [46], we employ a dynamic updating strategy to update λ_3 as $\lambda_3 \leftarrow \frac{2}{1+e^{-10\kappa}} - 1$, where κ starts from zero and increases with the iterative training process, making λ_3 gradually increase from 0 to 1. Lastly, we performed the network training for the weight in the auxiliary task L_{WR} with λ_4 increased from 0.01 to 0.1 with a step size of 0.01. Eventually, the optimal value of λ_4 in practice is 0.05.

TABLE I: The system parameters in O2 Dynamic Scenario in deepMIMO dataset [6].

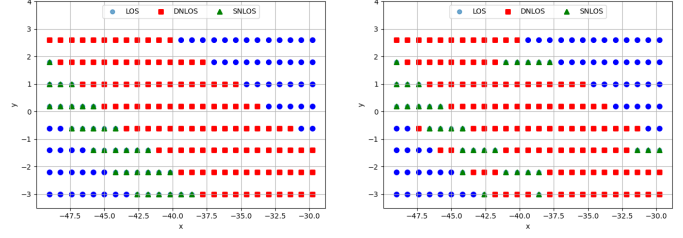
Parameters	Default Setting	Changeable Locations
Carrier Frequency	3.5 GHz	
Grid size	0.8m	
BS Location	(3,10,6)	
Subcarriers	64	
Antenna	8 × 8 Planar Array	Section V-D
MPCs	25	Section V-B and V-C1
Bandwidth	100 MHz	Section V-C2
Input type	ADP	Section V-D
Normalization	Antenna-wise	Section V-D2

2) On the Communication System and the Dataset:

The case studies are based on the Remcom 3D Ray-tracing dataset generated in the recently released dynamic outdoor scenario from the DeepMIMO website (<https://deepmimo.net/scenarios/o2-scenario/>). We focus on locating the UE(s) in a street canyon, especially the sidewalk of the main street. The main road has four lanes for mobile vehicles with different moving speeds, which change their positions for each data collection time. In this dataset, the minimum grid size (GS) for data collection is 0.2m. We use a GS of 0.8m by considering the trade-off between localization performance and data collection labor. It is noted that the vehicles have different sizes (e.g., sedans, trucks) and change their positions for each captured scene (channel realization). In the default setting, the UE can communicate with the BS with an 8 × 8 planar array antenna at 3.5 GHz carrier frequency with the bandwidth being 100 MHz. The maximum number of MPCs is 25. Tab. I summarizes default settings and change notes for communication system parameters in each case study.

Let $\mathbf{X} \in R^{L \times \Gamma \times M \times N}$ and $\mathbf{z} \in R^{L \times \Gamma \times 4}$ be the collected CSI (or its variants) and related labels (3D coordinates and propagation condition indicators), respectively. L , M , and N are the number of grid points, transmit antennas, and sub-carriers. Γ is the number of measured channel realizations at each location. We collect $\Gamma = 120$ scenes of data in the following experiments. "scene" here refers to a specific realization of moving blocking/scattering objects (cars) in the environment. For Wireless InSite software, we can capture CSIs from all L locations in one scene. For the default setting, the first fifty, next twenty, and last fifty scenes of CSI data are used for the neural network training, evaluation, and test, respectively. All datasets will be organized as a mini-batch during the network training process. We will store the optimal network models that obtained the best performance (RMSE) over the evaluation dataset and the corresponding epoch number for later convergence evaluation. In addition, we use the antenna-wise data normalization for the inputs, which are the angular delay profile (ADP) power matrix of CSI [13], [14]. The ADP is obtained from the CSI at the BS antenna elements by Fourier transformation and taking of the squared magnitude [11].

3) *Evaluation Protocols*: Given some estimates $\hat{\mathbf{z}}$, the root mean square errors (RMSEs) of the localization and accuracy of propagation condition prediction are



(a) Ground truth PCPs

(b) Estimated PCPs

Fig. 3: The ground truth and estimated PCPs (*Environmental Semantics*) in a sampled area.

denoted by:

$$RMSE = \frac{1}{L\Gamma} \sqrt{\sum_{l=1}^L \sum_{t=1}^{\Gamma} (x_{l,t} - \hat{x}_{l,t})^2 + (y_{l,t} - \hat{y}_{l,t})^2 + (z_{l,t} - \hat{z}_{l,t})^2}$$

and $Acc = \sum_{l,t} \delta(\hat{d}_{l,t} = d_{l,t}) / (L\Gamma)$, where $\delta(\cdot)$ denotes the indicator function.

In the following experiments, we compare the proposed methods (MDA and HDA) with three representative localization algorithms in the literature: 1) The deep convolutional neural network (DCNN) based supervised learning for end-to-end location estimation method [13]; this CNN-based end-to-end localization method uses ADP as input, and the related network structure [13] will be adopted as a backbone of feature extraction for all deep learning models. 2) the recently proposed localization method using unsupervised DA based transfer learning (TL) [53]; this method considers the distribution discrepancy caused by the dynamic environment and offers a scheme to overcome the feature space heterogeneity. 3) The scenario adaptive localization method with adversarial RDA technology, proposed in our conference paper [25], in which the invariant representation of the network input (fingerprints) was assured with an adversarial learning scheme. Unlike the proposed methods with CR and PCP tasks, DCNN only employed the labeled data to train the CR loss. Two transfer learning methods (TL and RDA) utilized unlabeled data and novel techniques to optimize the CR task.

B. Semantic Localization v.s. Standalone Localization

We first compare the semantic localization with the standalone one in terms of loss functions. The communication systems parameters are kept in same as the default setting in Tab. I, except for the available number of MPCs. To mimic the high dynamics in a street canyon, we assume that the number of MPCs (P in Eq.(1)) is a random variable, which obeys a uniform distribution $P \sim U(10, 25)$. Tab. II comprehensively compares each loss function in (7). For obtaining the importance weights (λ_1 and λ_2) in the supervised (dominant) learning task (CR and PCP), we use three optimization strategies: 1) Unweighted scheme, where we use equal importance $\lambda_1 = \lambda_2 = 0.5$; 2) Manual optimization scheme; 3) Uncertainty weighting scheme (as shown in Eq. (16)), in

Learning Task	Main Task Weight		KT Weight	Localization (RMSE)	Propagation Condition Prediction(PCP) (Accuracy)	Performance Gains (Localization/PCP)
Only Location Regression	1	0	✗	1.0567	-	-
	1	0	✓	0.9893	-	%6.813
Only Blockage Indication	0	1	✗	-	0.8772	-
	0	1	✓	-	0.9148	%4.286
Unweighted	0.5	0.5	✓	0.8802	0.9311	%20.05 /%6.145
Approx. Opt. (MDA)	0.7	0.3	✓	0.8299	0.9417	%27.33 /%7.353
Uncertainty weighting (HDA)	✓	✓	✓	0.8165	0.9359	%29.42 /%6.692

TABLE II: Quantitative experiments for each loss function in the proposed method. ✓/✗ means "with"/"without"; '-' means None. BP/KT denotes Blockage Prediction/Knowledge Transfer.

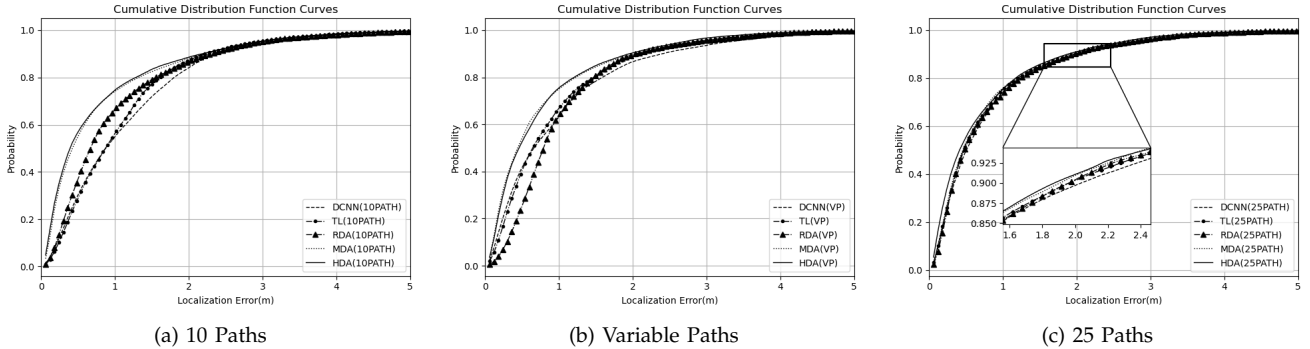


Fig. 4: The CDFs of localization errors for the three methods over different numbers of MPCs.

which the corresponding weights are denoted by the uncertainty measure and are optimized in the training process. Concerning the weights (λ_3 and λ_4) in KT (unsupervised learning) and WR losses, we follow the practical experience in the literature to get the corresponding optimal values.

The results in rows 2-4 of Tab. II show that joint training of the network with labeled and unlabeled data can boost CR and PCP performance, demonstrating the effectiveness of unsupervised DA methods. When comparing the results in the last three rows with the remainder, we find that the joint solution approach (semantic localization) consistently outperforms the localization-only solution. This can be explained by the fact that for the localization problem in the dynamic scenario, the propagation conditions between the BS and UE(s) change over time (see a sampled area in Fig.3a), making the localization more difficult. On the other hand, compared to the localization-only task, the semantic localization scheme jointly estimates the coordinates of the UE(s) and the related environmental semantics (PCPs in Fig.3b), which is a new dimension of the location information. This favorable information is used in the neural network designs (Section IV-A2). Moreover, the performance of the MDA method is sensitive to the importance of weights. Consequently, one might get inferior performance without optimization or fine-tuning of these weights, as verified by the results in the sixth row of Tab. II.

To get a genuine understanding of the effect of employed environmental semantics (PCPs), we show the localization performance in a selected sampled area

3a, including three kinds of PCPs (LOS, DNLOS, and SNLOS). DNLOS and SNLOS are NLOS propagation conditions caused by dynamic and static objects, respectively. We compared the proposed method (MDA) in three conditions: 1) Without using PCPs; 2) Using two kinds of PCPs: LOS and NLOS (DNLOS and SNLOS coexist); 3) Considering three kinds of PCPs. In the investigated area, the related RMSEs of the MDA in these three conditions are 0.6774m, 0.6032m, and 0.4234m, respectively. This case study result first proves that introducing environmental semantics recognition benefits localization. More importantly, distinguishing between static and dynamic scatterers significantly improves localization performance, as indicated by DNLOS and SNLOS indications. As a result, it is demonstrated that the more elaborate environmental semantics, the better localization performance one can have. Together with the novel neural network designs, the environmental semantics are used to reduce ambiguous features, thus enhancing the robustness of the localization algorithms against high environmental dynamics, which again explains the superiority of semantic localization.

In summary, the proposed semantic localization schemes significantly outperform standalone localization. Furthermore, integrating expert knowledge into the network optimization process improves localization accuracy. The uncertainty weighting helps to balance the different tasks in the semantic localization scheme and reduces the fine-tuning network complexity.

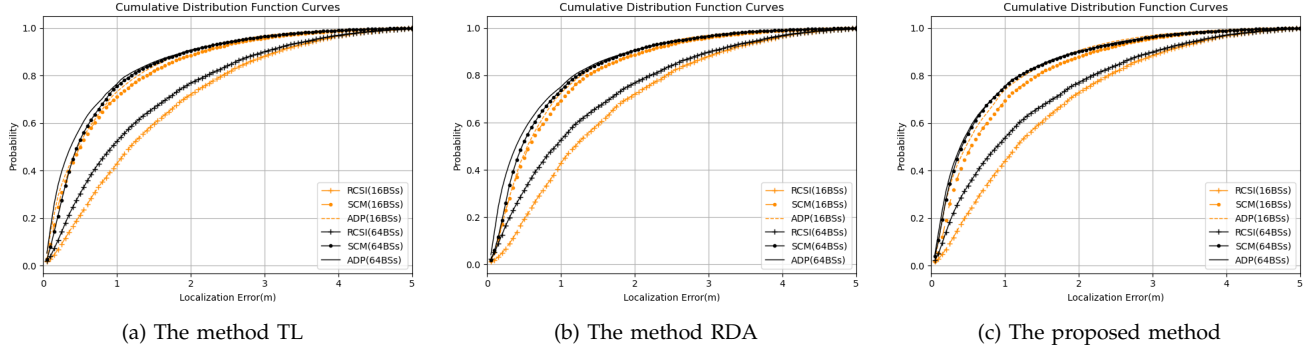


Fig. 5: The CDFs of RMSEs of different localization methods over different types of fingerprints and numbers of BS antennas.

C. Effect of Communication Systems Parameters

This group of experiments compares all localization methods with respect to the different communication systems configurations, such as the number of MPCs (Fig. 4) and the system bandwidth (Fig. 6).

1) *Impact of Number of MPCs*: We first investigate the performance of different localization methods in terms of the available number of MPCs P , for which we have three cases: 1) $P = 10$; 2) P is randomly selected from a uniform distribution $P \sim U(10, 25)$ for each channel realization; 3) $P = 25$ (Maximum in the DeepMIMO dataset). Fig. 4 shows the cumulative distribution function (CDF) of comparing the three representative localization methods, and all deep learning methods can obtain better localization performance with more MPCs. Besides, it is shown in Fig. 4a that TL performs better than the supervised DCNN method as it utilizes both labeled and unlabeled data. Fig. 4b illustrates that the proposed MDA has robust performance with respect to the variation in the number of MPCs. Moreover, the multi-task learning-based MDA outperforms the single-task learning-based TL, showing that 1) Employing unlabeled data improves both the accuracy and robustness of localization algorithms; 2) The multiple tasks localization methods do not harm the localization performance if we can have a proper scheme for importance weight of each task, demonstrating the effectiveness of semantic localization over classical localization in challenging dynamic environments.

2) *The Effect of the Bandwidth*: We next consider the impact of system bandwidth. We compare all employed localization methods for the dataset bandpass filtered with 20MHz and 100MHz communication systems. Other system configurations remain at their default settings (Tab. I). Fig. 6 illustrates that the system bandwidth is one of the critical parameters that affect the performance of localization algorithms. Compared to the localization method with only labeled data, the ones that jointly consider labeled and unlabeled data have significantly better performance, showing the effectiveness of adequately utilizing unlabeled data. Besides, the proposed multi-task MDA and HDA methods outperform the single-task

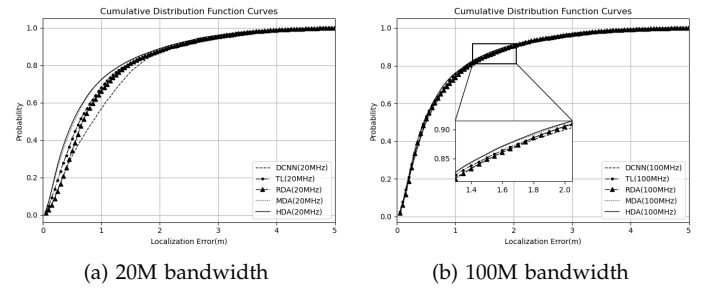


Fig. 6: The CDFs comparison of localization methods over different bandwidths

ones, showing the superiority of semantic localization over the classical ones again.

D. The Effect of the Utilization of Data

1) *Types of fingerprints*: This experiment shows the effect of the numbers of transmit antennas over three types of fingerprints: 1) Real-valued channel state information (RCSI); 2) Sample covariance matrix (SCM) of CSI measurements; 3) ADP power matrix. Fig. 5 shows a comparison of three DA methods in terms of CDF curves of the RMSE of localization. We used the default communication configuration to collect CSI data, except for the number of transmit antennas. It is shown in Fig. 5 that the number of transmit antennas is one of the critical factors for localization methods. The ADP-based localization methods obtain superior performance for both small and large numbers of transmit antennas, which can be explained by the fact that ADP preserves both the spatial and temporal ingredients of the CSI measurements while other employed fingerprints do not. Furthermore, for the 64-transmit-antenna communication system, the multi-task MDA localization with the SCM-based fingerprints can obtain comparable performance based on the ADP fingerprints, while other single-task localization methods cannot, showing the efficacy of semantic localization over the localization-only approach.

2) *The Effect of Data Normalization*: This experiment investigates the effect of four input data normalization schemes: 1) Antenna-wise (AW); 2) Sub-carrier wise

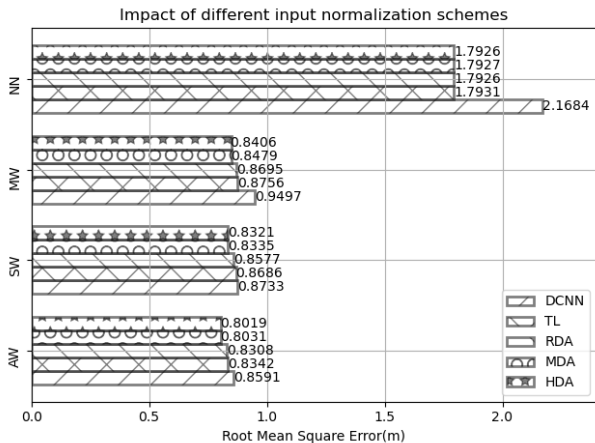


Fig. 7: A comparison of different localization methods over different input normalization schemes.

(SW); 3) Matrix-wise (MW); 4) No normalization (NN). The CSI data were collected under default communication configurations, as shown in Tab. I. We used the RMSE as the performance measure and ADP matrices as the inputs. Fig. 7 shows that data normalization is vital in all investigated localization methods. The localization methods with input data normalization attain at least two times less error than those without normalization. Furthermore, the AW scheme gives the best RMSE performance and slightly outperforms the SW one. Besides, these two data normalization strategies beat the MW one, showing the necessity of preserving the individualism of each antenna or subcarrier.

E. On the Convergence and Complexity

The complexities of deep learning-based localization methods [49], [54] are highly related to the convergence in the training stage, the model size, and the evaluation efficiency at the test stage. As a result, Tab. III reports the epoch (Epoch^{opt}) that the best evaluation performance happened during a total number of 2000 epochs training. Besides, at the test stage, we utilize the floating point operations per second (FLOPs) and the number of parameters (Para.) in the networks, which can be measured by the *thop* package from the Pytorch library. In Tab. III, we recorded the epochs to get the best performance over the validation dataset for all compared methods in a communication system with different numbers of MPCs. It is shown in Tab. III that the deep learning models consume more time (Epoch^{opt}) to converge when we have a more significant number of MPCs. This is reasonable as the available MPCs indicate complex wireless propagation conditions. Besides, the classical DCNN requires the least time to converge among all compared methods as it does not take advantage of unlabeled data. Moreover, the proposed MDA method requires the most extensive training time. In contrast, the proposed HDA is more efficient than MDA and performs similarly to the state-of-the-art DA-based localization methods, such

Methods	MPCs Number	Epoch ^{opt}	Test	
			Para.	FLOPs
DCNN	10 Paths	265	207.378K	8.801G
	VP	958		
	25 Paths	926		
TL	10 Paths	530	789.642K	17.699G
	VP	1383		
	25 Paths	1642		
RDA	10 Paths	443	273.556K	8.818G
	VP	1075		
	25 Paths	939		
MDA	10 Paths	1112	1.301M	17.830G
	VP	1604		
	25 Paths	1745		
HDA	10 Paths	631	1.301M	17.830G
	VP	1196		
	25 Paths	1023		

TABLE III: Complexity comparisons of all employed localization methods.

as RDA and TL, proving the necessity and superiority of the novel designs in HDA.

In summary, for space and evaluation efficiency consideration (Para. and FLOPs), Tab. III shows that the proposed MDA method requires more training to achieve their best performance for the joint task as they contain novel yet complicated designs in the knowledge transfer module. On the other hand, the proposed HDA is more efficient than the MDA and exists in state-of-the-art methods such as RDA. We note that the runtime (FLOPs) of the proposed MDA method increased by 0.74% compared to existing methods (TL [53]). These relatively small relative increases in cost are rewarded by a decrease of the localization error on the order of 30%, as verified in Tab. II. Regarding test performance (Para. and FLOPs), all deep learning localization methods have good complexity for many applications. The proposed methods obtain superior localization performance while consuming more memory budget and FLOPs.

VI. CONCLUSIONS

This paper investigated the challenging localization problem in an outdoor GPS-denied area with high dynamics. Compared to the classical localization setting, we first formulated the problem for semantic localization, taking advantage of fundamental propagation physics and improving the robustness against the high environmental dynamics. Moreover, we proposed two DA-based semantic localization algorithms: 1) The proposed MDA localization method integrates the wireless expert knowledge (scenario adaptive supervised learning and knowledge transfer) into the neural network design and optimization; 2) The proposed HDA localization algorithm improves the efficiency of the MDA by introducing the importance weights uncertainty modeling and the related maximum likelihood solution. Lastly, we conducted comprehensive experiments with a 3D ray tracing dataset. The case study results showed that 1) Compared to classical settings, the semantic localization

scheme gives better and more robust localization performance in a dynamic environment; 2) The component settings of the localization system, including communication system configurations, the neural network optimization schemes, and the utilization of input data, have a high impact on the localization results. The proposed localization methods offer more robust and precise results than existing ones over a wide range of experimental settings, demonstrating the benefits of applying the proposed algorithms for the accurate localizations of pedestrian/self-driving vehicles.

Throughout the case studies, it is found that environmental dynamics significantly affect the deep learning models. A proper scheme, such as the one in the proposed method, can be adopted to reduce the effect. However, it is worth exploiting the joint works integrating physics for channel modeling and the advantages of deep neural networks. Moreover, the related Doppler effect on the CSI data is no longer ignorable for a communication system with a very high carrying frequency, such as 30GHz or even higher. Lastly, verification of results based on actual measurements with a (hardware) channel sounder will be reported in future work.

APPENDIX A PROOF OF THEOREM 1

Since we have the assumption for the output of the CR network branch, we start proving the result in Theorem 1 by focusing on the likelihood function of the PCP network branch, which can be denoted by

$$p\left(\mathbf{y}_2 \mid \frac{1}{\sigma_2^2} h_{\mathcal{W}_2}(\mathbf{x})\right) = \text{softmax}\left(\frac{1}{\sigma_2^2} h_{\mathcal{W}_2}(\mathbf{x})\right), \quad (18)$$

where the related network parameter ensemble \mathcal{W}_2 was given in Section IV-A2 ($\mathcal{W}_2 = \{\Theta_1, \Theta_3\}$), and σ_2^2 is an auxiliary variable to denote the probability (temperature) rescaling level [52]. Eq.(18) boils down to the vanilla softmax function when $\sigma_2^2 = 1$. Suppose that the output of the softmax function gives the i -th class, then the corresponding log-likelihood yields

$$\log p(\mathbf{y}_2 = i \mid h_{\mathcal{W}_2}(\mathbf{x})) = \frac{1}{\sigma_2^2} \mathbf{u}_i - \log \sum_j \frac{1}{\sigma_2^2} \mathbf{u}_{ij}, \quad (19)$$

With some manipulation, we can simplify Eq.(19) as

$$\begin{aligned} & \log p\left(\mathbf{y}_2 = i \mid \frac{1}{\sigma_2^2} \mathbf{u}\right) \\ &= \frac{1}{\sigma_2^2} \left(\mathbf{u}_i - \sigma_2^2 \log \sum_j \exp\left(\frac{1}{\sigma_2^2} \mathbf{u}_{ij}\right) \right) \\ &= \frac{1}{\sigma_2^2} \left(\mathbf{u}_i - \log \left[\sum_j \exp(\mathbf{u}_{ij}) \right] \right) \\ &+ \left(\frac{1}{\sigma_2^2} \log \left(\sum_j \exp(\mathbf{u}_{ij}) \right) - \log \sum_j \exp\left(\frac{1}{\sigma_2^2} \mathbf{u}_{ij}\right) \right) \quad (20) \\ &= p(\mathbf{y}_2 \mid \mathbf{u}_i(\mathbf{x})) + \log \frac{(\sum_j \exp(\mathbf{u}_{ij}))^{\frac{1}{\sigma_2^2}}}{\sum_j \exp\left(\frac{1}{\sigma_2^2} \mathbf{u}_{ij}\right)} \\ &\stackrel{\text{assump.}}{\approx} \log \text{softmax}(\mathbf{u}_i) - \log \sigma_2^2 \end{aligned}$$

In Eq.(20), *assump.* denotes the case we have $\left(\sum_j \exp(\mathbf{u}_{ij})\right)^{\frac{1}{\sigma_2^2}} \approx \frac{1}{\sigma_2^2} \sum_j \exp\left(\frac{1}{\sigma_2^2} \mathbf{u}_{ij}\right)$, which becomes

an equality when $\sigma_2^2 \rightarrow 1$. With Assumption 2, we can have

$$\begin{aligned} & \log p(\mathbf{y}_1 \mid f_{\mathcal{W}_1}(\mathbf{x})) \\ &= \log \left(\frac{1}{\sigma_1 \sqrt{2\pi}} \exp\left(-\frac{1}{2} \frac{\|\mathbf{y}_1 - f_{\mathcal{W}_1}(\mathbf{x})\|^2}{\sigma_1^2}\right) \right) \quad (21) \\ &\propto -\frac{1}{2\sigma_1^2} \|\mathbf{y}_1 - f_{\mathcal{W}_1}(\mathbf{x})\|^2 - \log \sigma_1 \end{aligned}$$

Lastly, together with Eq.(20)-(21) and Assumption 2, we are ready to get the log-likelihood of the output of the neural network model ($q_{\mathcal{W}}(\mathbf{x})$):

$$\begin{aligned} & \log p(\mathbf{y}_1, \mathbf{y}_2 = i \mid q_{\mathcal{W}}(\mathbf{x})) \\ &= \log p(\mathbf{y}_1 \mid g_{\mathcal{W}_1}(\mathbf{x})) p(\mathbf{y}_2 = c \mid h_{\mathcal{W}_2}(\mathbf{x})) \\ &= \log p(\mathbf{y}_1 \mid g_{\mathcal{W}_1}(\mathbf{x})) p(\mathbf{y}_2 = c \mid h_{\mathcal{W}_2}(\mathbf{x})) \\ &\propto -\frac{1}{2\sigma_1^2} \|\mathbf{y}_1 - g_{\mathcal{W}_1}(\mathbf{x})\|^2 - \log \sigma_1 - \log \sigma_2^2 \\ &+ \frac{1}{\sigma_2^2} \log \text{softmax}(\mathbf{u}) \quad (22) \end{aligned}$$

which completes the proof of Theorem 1.

APPENDIX B THE PROOF OF COROLLARY 1

For the modulated CE loss (Eq. (9)), we are given a weighted conditional distribution function,

$$-\left(1 - p\left(\mathbf{y}_2 = c \mid \frac{1}{\sigma_2^2} \mathbf{u}\right)\right)^y \log p\left(\mathbf{y}_2 = c \mid \frac{1}{\sigma_2^2} \mathbf{u}\right), \quad (23)$$

where $\mathbf{u} = h_{\mathcal{W}_2}(\mathbf{x})$. Our goal here is to simplify the likelihood function $p\left(\mathbf{y}_2 = c \mid \frac{1}{\sigma_2^2} \mathbf{u}\right)$ and related log-likelihood function. Similar to Eq.(18), we have

$$\begin{aligned} & p\left(\mathbf{y}_2 = i \mid \frac{1}{\sigma_2^2} \mathbf{u}\right) = \text{softmax}\left(\frac{1}{\sigma_2^2} \mathbf{u}\right) \\ &= \frac{(\exp(\mathbf{u}_i))^{\frac{1}{\sigma_2^2}}}{\sum_j \exp\left(\frac{1}{\sigma_2^2} \mathbf{u}_{ij}\right)} \approx \frac{(\exp(\mathbf{u}_i))^{\frac{1}{\sigma_2^2}}}{\sigma_2^2 (\sum_j \exp(\mathbf{u}_{ij}))^{\frac{1}{\sigma_2^2}}} = \frac{1}{\sigma_2^2} (\text{softmax}(\mathbf{u}))^{\frac{1}{\sigma_2^2}}, \quad (24) \end{aligned}$$

Following the analysis shown in Eq.(20), we have

$$\begin{aligned} & \log p\left(\mathbf{y}_2 = i \mid \frac{1}{\sigma_2^2} \mathbf{u}\right) \\ &\approx \frac{1}{\sigma_2^2} \log p(\mathbf{y}_2 = c \mid \mathbf{u}) - \log \sigma_2^2 \\ &= \log \text{softmax}(\mathbf{u}) - \log \sigma_2^2 \quad (25) \end{aligned}$$

Plugging the results shown in Eq.(20) and Eq.(24) into Eq.(23) gives

$$\left(1 - \frac{1}{\sigma_2^2} (\text{softmax}(\mathbf{u}))^{\frac{1}{\sigma_2^2}}\right)^y \left(\log \text{softmax}(\mathbf{u}) - \log \sigma_2^2\right). \quad (26)$$

Similar to the analysis in Eq.(22), we arrive to the result in Eq.(16) with Eq.(21), Eq.(26), and Assumption 2.

REFERENCES

- [1] Y. Shen and M. Z. Win, "On the accuracy of localization systems using wideband antenna arrays," *IEEE Trans. Commun.*, vol. 58, no. 1, pp. 270-280, 2010.
- [2] O. Kanhere and T. S. Rappaport, "Position location for futuristic cellular communications: 5g and beyond," *IEEE Commun. Mag.*, vol. 59, no. 1, pp. 70-75, 2021.

- [3] G. Kwon, A. Conti, H. Park, and M. Z. Win, "Joint communication and localization in millimeter wave networks," *IEEE J. Sel. Top. Signal Process.*, vol. 15, no. 6, pp. 1439–1454, 2021.
- [4] A. Conti, F. Morselli, Z. Liu, S. Bartoletti, S. Mazuelas, W. C. Lindsey, and M. Z. Win, "Location awareness in beyond 5g networks," *IEEE Commun. Mag.*, vol. 59, no. 11, pp. 22–27, 2021.
- [5] A. Zappone, M. Di Renzo, and M. Debbah, "Wireless networks design in the era of deep learning: Model-based, ai-based, or both?" *IEEE Trans. Commun.*, vol. 67, no. 10, pp. 7331–7376, 2019.
- [6] A. Alkhateeb, "DeepMIMO: A generic deep learning dataset for millimeter wave and massive MIMO applications," in *Proc. of Information Theory and Applications Workshop (ITA)*, San Diego, CA, Feb 2019, pp. 1–8.
- [7] M. Alrabeiah and A. Alkhateeb, "Deep learning for mmwave beam and blockage prediction using sub-6 ghz channels," *IEEE Trans. Commun.*, vol. 68, no. 9, pp. 5504–5518, 2020.
- [8] Z. Li, K. Xu, H. Wang, Y. Zhao, X. Wang, and M. Shen, "Machine-learning-based positioning: A survey and future directions," *IEEE Network*, vol. 33, no. 3, pp. 96–101, 2019.
- [9] X. Zhu, W. Qu, T. Qiu, L. Zhao, M. Atiquzzaman, and D. O. Wu, "Indoor intelligent fingerprint-based localization: Principles, approaches and challenges," *IEEE Commun. Surv. Tutor.*, vol. 22, no. 4, pp. 2634–2657, 2020.
- [10] D. Burghal and etc., "A comprehensive survey of machine learning based localization with wireless signals," *ArXiv preprint*, 2023.
- [11] A. F. Molisch, *Wireless communications - From Fundamentals to Beyond 5G*, 3rd ed. IEEE Press - John Wiley & Sons, 2023.
- [12] X. Wang, L. Gao, S. Mao, and S. Pandey, "Deepfi: Deep learning for indoor fingerprinting using channel state information," in *IEEE WCNC*. IEEE, 2015, pp. 1666–1671.
- [13] J. Vieira, E. Leiting, and etc., "Deep convolutional neural networks for massive mimo fingerprint-based positioning," in *PIMRC*. IEEE, 2017, pp. 1–6.
- [14] X. Sun, X. Gao, and etc., "Single-site localization based on a new type of fingerprint for massive mimo-ofdm systems," *IEEE Trans. Veh. Technol.*, vol. 67, no. 7, pp. 6134–6145, 2018.
- [15] B. Mager, P. Lundrigan, and N. Patwari, "Fingerprint-based device-free localization performance in changing environments," *IEEE J. Sel. Areas Commun.*, vol. 33, no. 11, pp. 2429–2438, 2015.
- [16] S. J. Pan, J. T. Kwok, Q. Yang, and J. J. Pan, "Adaptive localization in a dynamic wifi environment through multi-view learning," in *AAAI*, vol. 7, 2007, pp. 1108–1113.
- [17] S. J. Pan, D. Shen, Q. Yang, and J. T. Kwok, "Transferring localization models across space." in *AAAI*, 2008, pp. 1383–1388.
- [18] Y. Zhang, A. Y. Ding, J. Ott, and etc., "Transfer learning-based outdoor position recovery with cellular data," *IEEE Trans. Mobile Comput.*, vol. 20, no. 5, pp. 2094–2110, 2020.
- [19] L. Li, X. Guo, and etc., "Transloc: A heterogeneous knowledge transfer framework for fingerprint-based indoor localization," *IEEE Trans. Wirel. Commun.*, vol. 20, no. 6, pp. 3628–3642, 2021.
- [20] F. Zhuang, Z. Qi, K. Duan, D. Xi, Y. Zhu, H. Zhu, H. Xiong, and Q. He, "A comprehensive survey on transfer learning," *Proc. IEEE*, vol. 109, no. 1, pp. 43–76, 2020.
- [21] X. Chen, H. Li, C. Zhou, X. Liu, D. Wu, and G. Dudek, "Fido: Ubiquitous fine-grained wifi-based localization for unlabelled users via domain adaptation," in *Proc. of The Web Conf.*, 2020, pp. 23–33.
- [22] G. Wang, A. Abbasi, and H. Liu, "Wifi-based environment adaptive positioning with transferable fingerprint features," in *IEEE CCWC*. IEEE, 2021, pp. 0123–0128.
- [23] X. Chen, H. Li, C. Zhou, X. Liu, D. Wu, and G. Dudek, "Fidora: Robust wifi-based indoor localization via unsupervised domain adaptation," *IEEE Internet Things J.*, 2022.
- [24] H. Li, X. Chen, J. Wang, D. Wu, and X. Liu, "Dafi: Wifi-based device-free indoor localization via domain adaptation," *Proc. ACM Interact. Mob. Wearable Ubiquitous Technol.*, vol. 5, no. 4, pp. 1–21, 2021.
- [25] L. Chu, A. Alghafis, and A. F. Molisch, "SA-Loc: Scenario adaptive localization in highly dynamic environment using adversarial regressive domain adaptation," in *IEEE RFID*, 2022, pp. 132–137.
- [26] R. Zhou, H. Hou, Z. Gong, Z. Chen, K. Tang, and B. Zhou, "Adaptive device-free localization in dynamic environments through adaptive neural networks," *IEEE Sens. J.*, vol. 21, no. 1, pp. 548–559, 2020.
- [27] Y. Tian, J. Wang, and Z. Zhao, "Wi-fi fingerprint update for indoor localization via domain adaptation," in *IEEE ICPADS*. IEEE, 2021, pp. 835–842.
- [28] J. L. Schönberger, M. Pollefeys, A. Geiger, and T. Sattler, "Semantic visual localization," in *IEEE CVPR*, 2018, pp. 6896–6906.
- [29] A. Bourdoux, A. N. Barreto, and etc., "6g white paper on localization and sensing," *arXiv preprint arXiv:2006.01779*, 2020.
- [30] Y. Lin, D. Jiang, and etc., "Locator: cleaning wifi connectivity datasets for semantic localization," *Proc. VLDB Endow.*, vol. 14, no. 3, pp. 329–341, 2020.
- [31] M. Weber and E. A. Lee, "Semantic localization for iot," in *Semantic IoT: Theory and Applications*, 2021, pp. 365–383.
- [32] H. Tataria, M. Shafi, A. F. Molisch, and etc., "6g wireless systems: Vision, requirements, challenges, insights, and opportunities," *Proc. IEEE*, vol. 109, no. 7, pp. 1166–1199, 2021.
- [33] C. Huang, A. F. Molisch, R. He, R. Wang, P. Tang, B. Ai, and Z. Zhong, "Machine learning-enabled los/nlos identification for mimo systems in dynamic environments," *IEEE Trans. Wireless Commun.*, vol. 19, no. 6, pp. 3643–3657, 2020.
- [34] R. Zekavat and R. M. Buehrer, *Handbook of position location: Theory, practice and advances, 2nd Edition*. John Wiley & Sons, 2019, vol. 27.
- [35] T. Choi, F. Rottenberg, and etc., "Experimental investigation of frequency domain channel extrapolation in massive mimo systems for zero-feedback fdd," *IEEE Trans. Wireless Commun.*, vol. 20, no. 1, pp. 710–725, 2020.
- [36] J. A. Fessler and A. O. Hero, "Space-alternating generalized expectation-maximization algorithm," *IEEE Trans. Signal Process.*, vol. 42, no. 10, pp. 2664–2677, 1994.
- [37] M. Wax and A. Leshem, "Joint estimation of time delays and directions of arrival of multiple reflections of a known signal," *IEEE Trans. Signal Process.*, vol. 45, no. 10, pp. 2477–2484, 1997.
- [38] G. G. Raleigh and T. Boros, "Joint space-time parameter estimation for wireless communication channels," *IEEE Trans. Signal Process.*, vol. 46, no. 5, pp. 1333–1343, 1998.
- [39] M. D. Larsen, A. L. Swindlehurst, and T. Svantesson, "Performance bounds for mimo-ofdm channel estimation," *IEEE Trans. Signal Process.*, vol. 57, no. 5, pp. 1901–1916, 2009.
- [40] F. Wen, P. Liu, H. Wei, Y. Zhang, and R. C. Qiu, "Joint azimuth, elevation, and delay estimation for 3-d indoor localization," *IEEE Trans. Veh. Technol.*, vol. 67, no. 5, pp. 4248–4261, 2018.
- [41] N. Hernández, J. M. Alonso, and M. Ocaña, "Fuzzy classifier ensembles for hierarchical wifi-based semantic indoor localization," *Expert Syst. Appl.*, vol. 90, pp. 394–404, 2017.
- [42] M. Steinbauer, A. F. Molisch, and E. Bonek, "The double-directional radio channel," *IEEE Antennas Propag. Mag.*, vol. 43, no. 4, pp. 51–63, 2001.
- [43] G. Wilson and D. J. Cook, "A survey of unsupervised deep domain adaptation," *ACM Trans. Intell. Syst. Technol.*, vol. 11, no. 5, pp. 1–46, 2020.
- [44] N. Tripuraneni, M. Jordan, and C. Jin, "On the theory of transfer learning: The importance of task diversity," *Proc. Adv. Neural Inf. Process. Syst.*, vol. 33, pp. 7852–7862, 2020.
- [45] T.-Y. Lin, P. Goyal, R. Girshick, K. He, and P. Dollár, "Focal loss for dense object detection," in *IEEE ICCV*, 2017, pp. 2980–2988.
- [46] M. Long, Z. Cao, J. Wang, and M. I. Jordan, "Conditional adversarial domain adaptation," *NeurIPS*, vol. 31, 2018.
- [47] K. Saito, Y. Ushiku, T. Harada, and K. Saenko, "Strong-weak distribution alignment for adaptive object detection," in *IEEE CVPR*, 2019, pp. 6956–6965.
- [48] L. Song, J. Huang, A. Smola, and K. Fukumizu, "Hilbert space embeddings of conditional distributions with applications to dynamical systems," in *ICML*, 2009, pp. 961–968.
- [49] I. Goodfellow, Y. Bengio, and A. Courville, "Regularization for deep learning," *Deep learning*, pp. 216–261, 2016.
- [50] A. Kendall and Y. Gal, "What uncertainties do we need in bayesian deep learning for computer vision?" *Proc. Adv. Neural Inf. Process. Syst.*, vol. 30, 2017.
- [51] M. I. Jordan, Z. Ghahramani, T. S. Jaakkola, and L. K. Saul, "An introduction to variational methods for graphical models," *Machine learning*, vol. 37, no. 2, pp. 183–233, 1999.
- [52] C. Guo, G. Pleiss, Y. Sun, and K. Q. Weinberger, "On calibration of modern neural networks," in *ICML*. PMLR, 2017, pp. 1321–1330.
- [53] L. Li, X. Guo, Y. Zhang, N. Ansari, and H. Li, "Long short-term indoor positioning system via evolving knowledge transfer," *IEEE Trans. Wireless Commun.*, vol. 21, no. 7, pp. 5556–5572, 2022.
- [54] L. Deng, D. Yu et al., "Deep learning: methods and applications," *Found. Trends Signal Process.*, vol. 7, no. 3–4, pp. 197–387, 2014.